JOURNAL OF MAGNETIC RESONANCE **127,** 128–133 (1997)
ARTICLE NO. MN971199

COMMUNICATION

Determination of Amide Proton CSA in ^{15}N-Labeled Proteins Using ^{1}H CSA/^{15}N–^{1}H Dipolar and ^{15}N CSA/^{15}N–^{1}H Dipolar Cross-Correlation Rates

Marco Tessari, Frans A. A. Mulder, Rolf Boelens, and Geerten W. Vuister*

Department of NMR Spectroscopy, Bijvoet Center for Biomolecular Research, Utrecht University, Padualaan 8, 3584 CH Utrecht, The Netherlands

Received March 31, 1997; revised May 20, 1997

Knowledge of the magnitude and orientation of the amide-proton chemical shift anisotropy (CSA) is of great interest because of its correlation with hydrogen bonding and secondary structure (*1*). Information about the CSA of amide protons can be obtained from solid-state NMR measurements, but so far only a few experimental observations have been reported limited to small synthetic ^{15}N-labeled peptides and organic molecules (*2–5*). An alternative approach employs the measurement of cross-correlation effects in solution between the amide-proton CSA and amide-proton-^{15}N dipolar interactions ($^{1}H^{N}$ CSA/DD). The CSA/DD cross correlation contains information on the motional properties and the anisotropy of the chemical shift tensor (*6–12*). Earlier, we showed how quantitative measurement of the $^{1}H^{N}$ CSA/DD cross-correlation rates can be combined with the results obtained from ^{15}N relaxation studies to yield information about the magnitude of the $^{1}H^{N}$ CSA (*1*). Here, we present an alternative approach for extracting the $^{1}H^{N}$ CSA using both the $^{1}H^{N}$ CSA/DD and the ^{15}N CSA/DD (^{15}N CSA/$^{1}H^{N}$-^{15}N dipolar) cross-correlation rates, which alleviates the need for an extensive ^{15}N relaxation study. Recently, Tjandra *et al.* (*13*) proposed an experiment for quantitative measurement of the ^{15}N CSA/DD cross-correlation rates in ^{15}N-labeled proteins. Here, we use an alternative experiment which yields a linear buildup of the ^{15}N CSA/DD cross-correlation effect, rather than a hyperbolic tangent, and employs a different scheme for removing the (large) unwanted coherences.

The pulse sequence for the quantitative measurement of the ^{15}N CSA/DD cross correlation is shown in Fig. 1A. Two spectra are recorded: one in which the operator terms arising from ^{15}N CSA/DD cross correlation are selected and a reference experiment. The pulse scheme is set up as a constant-time experiment in which the reference experiment is (virtually) free of ^{15}N CSA/DD relaxation interference effects.

At time point *a* in the sequence, antiphase ^{15}N magnetization, $2\mathbf{I}_z\mathbf{S}_y$, has been created where **I** and **S** denote the $^{1}H^{N}$ and ^{15}N spin operators of the product-operator formalism (*14*), respectively. In the presence of ^{15}N CSA/DD cross-correlation the antiphase ^{15}N magnetization will be partially converted to in-phase ^{15}N magnetization (*8, 10, 11, 13*) so that at time point *b* the following terms are generated:

$$\begin{aligned} 2\mathbf{I}_z\mathbf{S}_y \xrightarrow{4T} & 2\mathbf{I}_z\mathbf{S}_y \exp[-4\lambda(T-\Delta)] \\ & \times \{E(+,4\Delta)+E(-,4\Delta)\}/2 \\ & + \mathbf{S}_y \exp[-4\lambda(T-\Delta)] \\ & \times \{E(+,4\Delta)-E(-,4\Delta)\}/2, \quad [1] \end{aligned}$$

where $E(\pm,\tau)$ is defined as $\exp\{-(\lambda \pm \eta_N)\tau\}$ and λ and η_N denote the auto-relaxation and cross-correlation rates (cf. Eqs. [9] and [10]), respectively (*8, 13*). Evolution due to ^{15}N chemical shift and ^{15}N–$^{1}H^{N}$ heteronuclear J coupling is refocused at time point *b*. The $90°(\phi_8, \mathbf{I})$, $90(\phi_6, \mathbf{S})$ pulses do not affect the $\mathbf{S}_y$ term, whereas the $2\mathbf{I}_z\mathbf{S}_y$ operator is converted into multiple-quantum terms:

$$\begin{aligned} [1] \xrightarrow{90°(\phi_8,\mathbf{I}),\ 90(\phi_6,\mathbf{S})} & -2\mathbf{I}_y\mathbf{S}_y \exp[-4\lambda(T-\Delta)] \\ & \times \{E(+,4\Delta)+E(-,4\Delta)\}/2 \\ & + \mathbf{S}_y \exp[-4\lambda(T-\Delta)] \\ & \times \{E(+,4\Delta)-E(-,4\Delta)\}/2. \quad [2] \end{aligned}$$

* To whom correspondence should be addressed.

1090-7807/97 $25.00

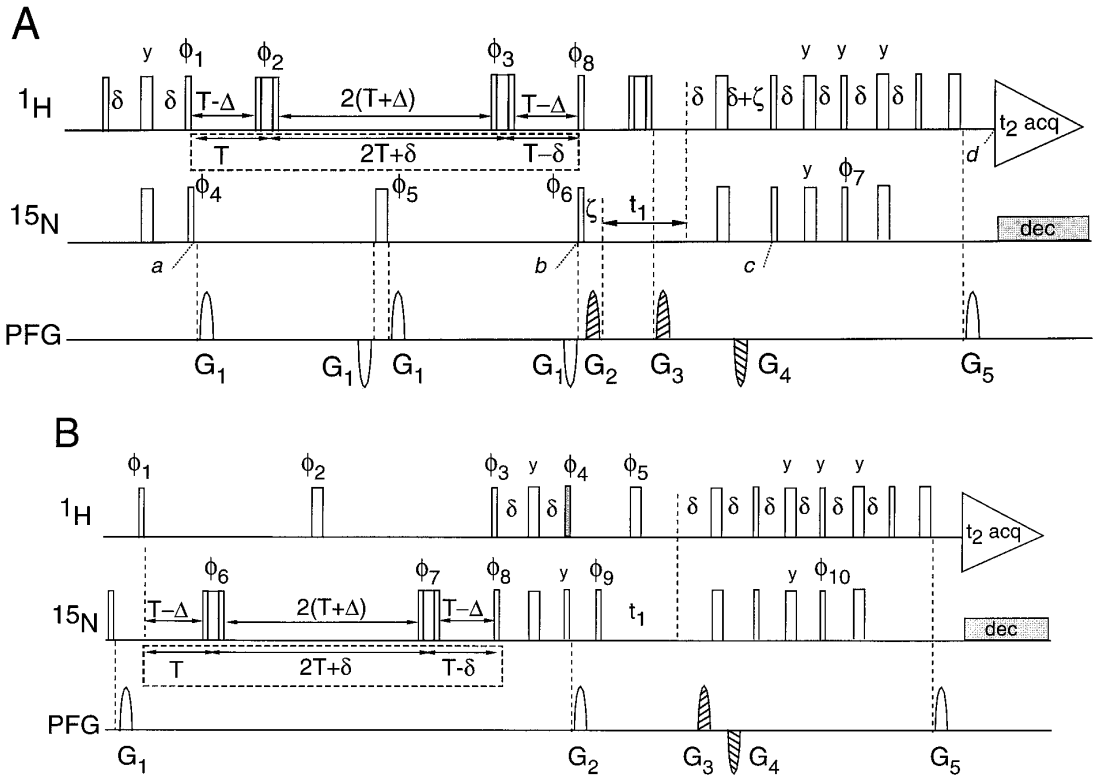

FIG. 1. Pulse sequences for quantitative measurement of ^{15}N CSA/DD cross-correlation rates (A) and $^{1}H^{N}$ CSA/DD cross-correlation rates (B) (*1*). Narrow and wide bars denote pulses with a 90° and 180° flip angle, respectively. For both experiments, two variations of the pulse scheme are recorded selecting for magnetization arising from CSA/DD pathways and a reference. For the reference experiment the delays were chosen as indicated in the dashed boxes and the phase ϕ_6 (A) or ϕ_3 (B) was changed. All pulsed-field gradients (PFG) had a sine-bell shape and were applied along the *z* axis. In order to record P- and N-type spectra using the sensitivity-enhanced gradient-coherence selection in the manner described by Kay *et al.* (*15*), hatched gradients are alternated in sign together with incrementing ϕ_7 (A) or ϕ_{10} (B) by 180° on successive FIDs. Post-acquisition data processing yields cosine- and sine-modulated data in t_1 ^{15}N decoupling during acquisition was accomplished using WALTZ-16 decoupling scheme (*18*) with an RF field strength of 1.25 kHz. Delay durations: $\delta = 2.7$ ms; $4\Delta = 0$ (reference), 10.8, 21.6 ms. (A) Phase cycling: $\phi_1 = y, -y$; $\phi_2 = 64x, 64(-x)$; $\phi_3 = 8y, 8(-y)$; $\phi_4 = 8(-x), 8x$; $\phi_5 = 2x, 2y, 2(-x), 2(-y)$; $\phi_6 = 32y, 32(-y)$ (CSA/DD) or $32x, 32(-x)$ (reference); $\phi_7 = y$; $\phi_8 = 16x, 16(-x)$; receiver = $2P, 4(-P), 2P$ with P = $(x, -x, -x, x)$. Duration and strength of the gradients: $G_1 = 1$ ms, −6.6 G/cm; $G_2 = 1$ ms, −10 G/cm; $G_3 = 1$ ms, −30 G/cm; $G_4 = 2.0$ ms, 20 G/cm; and $G_5 = 1$ ms, 8.112 G/cm. Delays, $T = 6.5$ ms; $\zeta = G_2 + 100$ μs. (B) The gray-colored ^{1}H 90°(ϕ_4) pulse is applied only in the reference experiment in order to move the water magnetization back to the +*z* axis. Phase cycling: $\phi_1 = 2(-x), 2x$; $\phi_2 = y, -y, x, -x$; $\phi_3 = x$ or $\phi_3 = y, -y$ (reference); $\phi_4 = 2x, 2(-x)$ (reference only); $\phi_5 = 16x, 16(-x)$; $\phi_6 = 16x, 16(-x)$; $\phi_7 = 32x, 32(-x)$; $\phi_8 = 4x, 4(-x)$; $\phi_9 = 8x, 8(-x)$; $\phi_{10} = y$; Receiver = $4x, 8(-x), 4x$ or Receiver = $2(x, -x), 4(-x, x), 2(x, -x)$ (reference). Duration and strength of the gradients: $G_1 = 2$ ms, 15 G/cm; $G_2 = 1$ ms, 20 G/cm; $G_3 = 2$ ms, −20 G/cm; $G_4 = 2.0$ ms, 20 G/cm; and $G_5 = 1$ ms, 8.112 G/cm. Delay, $T = 5.4$ ms.

During the subsequent delays $t_1 + 2\delta + 2\zeta$ (between time points *b* and *c*) the $\mathbf{S}_y$ term is labeled with its chemical shift and becomes antiphase with respect to the I-spin. A suitable choice of gradients G_2, G_3, G_4, and G_5 selects either P- or N-type coherence which is transferred to the I-spin using gradient-coherence selection with sensitivity-enhancement as proposed by Kay *et al.* (*15*). The (large) unwanted $2\mathbf{I}_y\mathbf{S}_y$ multiple-quantum term is effectively dephased by the gradients G_2, G_3, and G_4 and does not lead to observable magnetization.

Hence, neglecting all constant factors resulting from evolution between time points *c* and *d*, the resulting signal at the start of t_2 (timepoint *d*) can be described by

$$\begin{aligned} S^{\text{cross}}(t_1, t_2) = \langle \mathbf{I}_+ \rangle &\exp[-4\lambda(T - \Delta)] \\ &\times \{E(+, 4\Delta) - E(-, 4\Delta)\}/2 \\ &\times \sin(2\pi^1 J_{\text{NH}}\delta)\exp(\pm i\omega_{\text{N}} t_1) \\ &\times \exp(-i\omega_{\text{H}} t_2), \end{aligned} \quad [3]$$

where $\exp(\pm i\omega_{\text{N}} t_1)$ describes the ^{15}N chemical shift evolution resulting from either P- or N-type coherence selection.

Under the experimental conditions chosen, the $\sin(2\pi^1 J_{NH}\delta)$ term can be safely equated to 1 so that after linear combination of the P- and N-type FIDs and two-dimensional Fourier transformation, the intensity of the peak resulting from the ^{15}N CSA/DD mechanism, I^{cross}, is equal to

$$I^{cross} = C \exp[-4\lambda(T - \Delta)] \times \{E(+, 4\Delta) - E(-, 4\Delta)\}, \quad [4]$$

where C denotes a proportionality constant resulting from constant factors, experimental setup, and processing.

For the reference experiment, Δ is chosen zero and the 180°(ϕ_3, **I**) pulse is offset by an amount δ, as indicated in the boxed area of Fig. 1. The antiphase S operator present at time point *a* now evolves as

$$\begin{aligned} 2\mathbf{I}_z\mathbf{S}_y \xrightarrow{4T} & -\mathbf{S}_x \exp[-\lambda(4T - 2\delta)] \\ & \times \{E(+, 2\delta) + E(-, 2\delta)\}/2 \sin(2\pi^1 J_{NH}\delta) \\ & - 2\mathbf{I}_z\mathbf{S}_x \exp[-\lambda(4T - 2\delta)] \\ & \times \{E(+, 2\delta) - E(-, 2\delta)\}/2 \sin(2\pi^1 J_{NH}\delta). \end{aligned} \quad [5]$$

Again, the 90°(ϕ_8, **I**), 90(ϕ_6, **S**) pulses, with ϕ_6 now shifted by 90°, do not affect the $\mathbf{S}_x$ term, whereas the $2\mathbf{I}_z\mathbf{S}_x$ operator is converted into a multiple-quantum operator. The remainder of the pulse scheme has been described above, so that the unwanted term is again dephased by the gradients G_2, G_3, and G_4. Note that in the scheme of Tjandra *et al.* (*13*) the cross-relaxation experiment requires the application of additional pulses relative to the reference scheme.

At the start of t_2 (time point *d*) the signal is now described by

$$\begin{aligned} S^{ref}(t_1, t_2) = & \langle \mathbf{I}_+ \rangle \exp[-\lambda(4T - 2\delta)] \\ & \times \{E(+, 2\delta) + E(-, 2\delta)\}/2 \\ & \times \sin^2(2\pi^1 J_{NH}\delta) \exp(\pm i\omega_N t_1) \\ & \times \exp(-i\pi/2) \exp(-i\omega_H t_2), \end{aligned} \quad [6]$$

where the $\exp(-i\pi/2)$ factor results from the presence of the $-\mathbf{S}_x$ operator at the start of t_1. After linear combination of the P- and N-type FIDs, two-dimensional Fourier transformation, and appropriate phasing, the intensity of the reference peak, I^{ref}, equating $\sin^2(2\pi^1 J_{NH}\delta)$ to 1, becomes

$$I^{ref} = -C \exp(-\lambda[4T - 2\delta]) \{E(+, 2\delta) + E(-, 2\delta)\}. \quad [7]$$

Since $4\Delta\eta_N \ll 1$, the intensity ratio of the ^{15}N CSA/DD cross-peak to the reference cross-peak can be written as

$$I^{cross}/I^{ref} \approx 4\Delta\eta_N, \quad [8]$$

which shows the linear dependence of this ratio on Δ and the cross-correlation rate η_N. As was the case for the measurement of the ^{1}H^N CSA/DD cross-correlation rate (*1*), the linear approximation of Eq. [8] holds true for values of 4Δ that largely exceed λ^{-1}, even for a large η_N/λ ratio of 0.25.

Assuming axial symmetry for the CSA interaction, the ^{15}N relaxation rates for auto-relaxation, λ, and cross-correlation, η_N, can be expressed in terms of the spectral densities for dipolar auto-correlation, $J^{dd}(\omega)$, CSA auto-correlation, $J^{cc}(\omega)$, and CSA/dipolar cross-correlation, $J^{cd}(\omega)$, as (*8, 13*)

$$\begin{aligned} \lambda = D[& 4J^{dd}(0) + 4\alpha_N{}^2 J^{cc}(0) + 3\alpha_N{}^2 J^{cc}(\omega_H) \\ & + 3J^{dd}(\omega_H) + 3J^{dd}(\omega_H - \omega_N) + 3J^{dd}(\omega_N) \\ & + 6J^{dd}(\omega_H + \omega_N)] \end{aligned} \quad [9]$$

and

$$\eta_N = 2\alpha_N D[4J^{cd}(0) + 3J^{cd}(\omega_N)] \quad [10]$$

with

$$D = 1/8(\mu_0/4\pi)^2(\gamma_N\gamma_H\hbar r_{NH}^{-3})^2 \quad [11a]$$

and

$$\alpha_N = -2/3(4\pi/\mu_0)B_0(\sigma_\parallel^N - \sigma_\perp^N)r_{NH}^3/(\hbar\gamma_H) \quad [11b]$$

and where α_N is defined as the ratio of the strength of CSA and dipolar interaction, r_{NH} denotes the ^{15}N–^{1}H^N internuclear distance, taken to be 1.02 Å, B_0 denotes the static field, and $\sigma_\parallel^N$ and $\sigma_\perp^N$ denote the parallel and perpendicular components of the ^{15}N chemical shielding tensor, respectively. For a rigid molecule with isotropic rotational diffusion the following relations among the $J^{dd}(\omega)$, $J^{cc}(\omega)$, and $J^{cd}(\omega)$ terms hold (*11*)

$$\begin{aligned} J^{dd}(\omega) &= J^{cc}(\omega) \\ &= J^{cd}(\omega)/[(3\cos^2\theta_N - 1)/2] = J(\omega), \end{aligned} \quad [12]$$

where θ_N denotes the angles between the symmetry axes of CSA and dipolar tensors. In the presence of internal motion that can be described by equivalent independent restricted rotations around three mutually orthogonal axes, Eq. [12] is

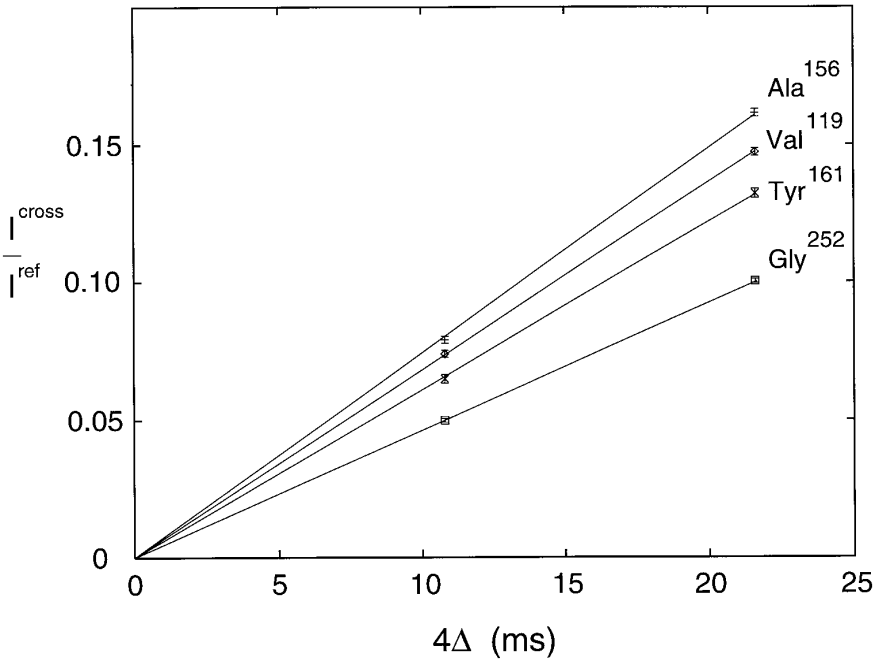

FIG. 2. Buildup of the I^{cross}/I^{ref} ratios as a function of 4Δ for Val^{119}, Ala^{156}, Tyr^{161}, and Gly^{252} of savinase.

still a very good approximation for small angles of θ_N (*13*), in which case Eq. [10] reduces to

$$\eta_N = 2\alpha_N D[4J(0) + 3J(\omega_N)](3\cos^2\theta_N - 1)/2. \quad [13]$$

The NMR experiments were performed at 315 K on a 2 m*M* solution of uniformly ^{15}N-labeled serine protease savinase (*19*) in 95/5, v/v, H_2O/D_2O solution in the presence of 25 m*M* acetate at pH 5.0. The ^{15}N CSA/DD and $^1H^N$ CSA/DD cross-correlation rates were measured using the pulse sequences of Fig. 1A and Fig. 1B (*1*), respectively, on a Varian Unity*Plus* spectrometer equipped with a triple-resonance probe with a shielded *z*-gradient coil operating at 499.91 MHz ^1H resonance frequency. For both the ^{15}N and $^1H^N$ CSA/DD experiments, a reference and 2 CSA/DD data sets were recorded in an interleaved fashion using delay values 4Δ of 10.8, and 21.6 ms, respectively. The ^{15}N CSA/DD experiment was repeated four times and the $^1H^N$ CSA/DD was repeated once to check the reproducibility of the resulting data. For the analysis, all data sets were used. All spectra consisted of 128 (t_1) × 768 (t_2) complex points with maximum acquisition times of 64 (t_1) and 76.8 (t_2) ms. All data were processed using NMRPipe and analyzed using both in-house written software as well as the nlinLS nonlinear least-squares minimization tool of the NMRPipe software package (*16*).

The experiment displayed in Fig. 1A was used to measure the ^{15}N CSA/DD cross-correlation rates on a 2 m*M* solution in H_2O of uniformly ^{15}N-labeled savinase. Figure 2 shows the I^{cross}/I^{ref} ratios for residues Val^{119}, Ala^{156}, Tyr^{161}, and Gly^{252} as a function of 4Δ as obtained from the ^{15}N CSA/DD cross-correlation data. Repetition of the experiment indicated a very good reproducibility, with I^{cross}/I^{ref} ratios being identical within the experimental error resulting from the thermal noise in the CSA/DD and reference spectra. In contrast to an earlier experiment proposed for quantitative measurement of ^{15}N CSA/DD cross-correlation rates (*13*), the present experiment yields linear buildups, rather than a hyperbolic tangent. Thus, extraction of the cross-correlation rates, η_N, is straightforward and can be done by a simple one-parameter linear fit. At 11.7 T, we thus obtain 6.8, 7.4, 6.1, and 4.6 s^{-1} for Val^{119}, Ala^{156}, Tyr^{161}, and Gly^{252}, respectively. Overall, for 210 residues of savinase showing nonoverlapping correlations in the $^1H^N$–^{15}N spectrum it was possible to extract those rates which fall in the range 4.5–7.5 s^{-1} at 11.7 T with an average of 6.6 ± 0.5 s^{-1}. These values are shown as a function of residue number in Fig. 3A. The ^{15}N CSA/DD rates are rather uniform, which corroborates the finding from ^{15}N relaxation studies on serine proteases of this family which indicate a globular, well-structured, isotropic tumbling protein displaying similar dynamics for most residues (*17*, F. A. A. Mulder, unpublished results).

$^1H^N$ CSA/DD rates, η_H, were also measured for this enzyme using the experiment of Fig. 1B, which was described in detail previously (*1*). Figure 3B shows these rates as a function of residue number. It is immediately apparent that they show a much larger range, varying between 1.0 and

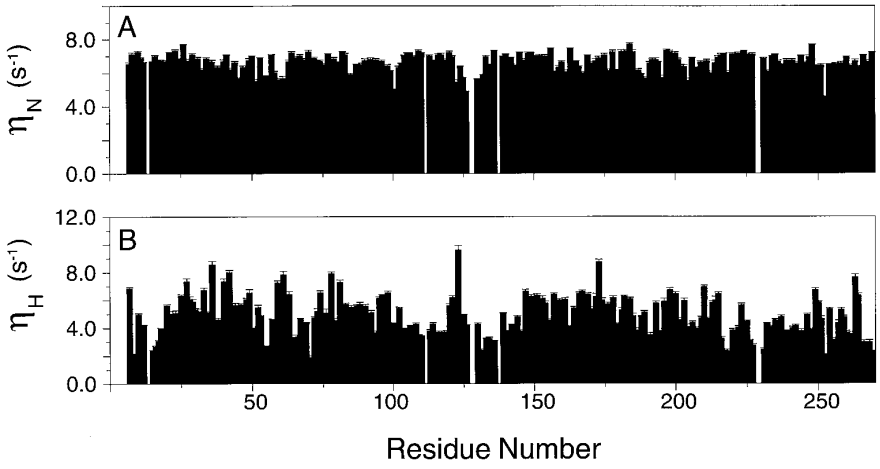

FIG. 3. ^{15}N CSA/DD cross-correlation rates, η_N (A), and $^1H^N$ CSA/DD cross-correlation rates, η_H (B), as a function of residue number in savinase.

9.5 s^{-1} with an average of 4.7 ± 1.5 s^{-1}. The $^1H^N$ CSA/DD rates are dependent upon the CSA of the amide proton and also on the mobility of the $^1H^N$–^{15}N bond vector (*8, 13*)

$$\eta_H = 2\alpha_H D[4J(0) + 3J(\omega_H)](3\cos^2\theta_H - 1)/2, \quad [14]$$

where θ_H denotes the angle between the symmetry axes of the $^1H^N$ CSA and dipolar tensors, D is defined as before (cf. Eq. [11a]), and α_H is defined as

$$\alpha_H = -2/3(4\pi/\mu_0)B_0(\sigma_\parallel^H - \sigma_\perp^H)r_{NH}^3/(\hbar\gamma_N), \quad [15]$$

where $\sigma_\parallel^H$ and $\sigma_\perp^H$ denote the parallel and perpendicular components of the ^{1}H chemical shielding tensor, respectively.

Using Eqs. [11a], [12], [14], and [15], the $^1H^N$ CSA/DD rates can be used to calculate $\Delta\sigma_H^*$, which equals $(\sigma_\parallel^H - \sigma_\perp^H)(3\cos^2\theta_H - 1)/2$, if the spectral density terms $J(0)$ and $J(\omega_H)$ are known from ^{15}N relaxation studies. The alternative approach proposed here uses both the $^1H^N$ CSA/DD and ^{15}N CSA/DD cross correlation rates. After substitution of the appropriate constants the ratio of these rates, η_H/η_N, can be written as

$$\eta_H/\eta_N = (\gamma_H/\gamma_N)(\Delta\sigma_H^*/[(\sigma_\parallel^N - \sigma_\perp^N)(3\cos^2\theta_N - 1)/2]) \times [4J(0) + 3J(\omega_H)]/[4J(0) + 3J(\omega_N)]. \quad [16]$$

At 315 K, savinase has a rotational correlation time of ~9 ns (F. A. A. Mulder, unpublished results). Consequently, $J(\omega_N)$ and $J(\omega_H)$ are one and three orders of magnitude smaller than $J(0)$, respectively, and therefore they can be neglected from Eq. [16]. Earlier studies on ubiquitin indicated that the $(\sigma_\parallel^N - \sigma_\perp^N)(3\cos^2\theta_N - 1)/2$ term is rather uniform and is equal to −145.6 ppm (*13*). Using this value and neglecting $J(\omega_N)$ and $J(\omega_H)$, $\Delta\sigma_H^*$ can be expressed in terms of the η_H/η_N ratio:

$$\Delta\sigma_H^* = (\eta_H/\eta_N) \times 14.7 \text{ ppm}. \quad [17]$$

Figure 4 shows the values for $\Delta\sigma_H^*$ calculated using Eqs. [11a], [12], [14], [15], and the $J(0)$ values obtained from reduced spectral density mapping *vs* the values for $\Delta\sigma_H^*$ calculated using Eq. [17]. The correlation between the two

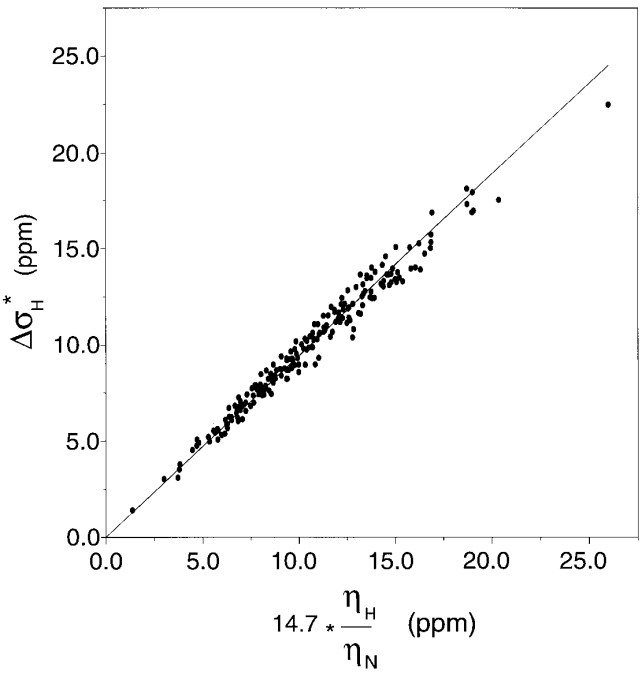

FIG. 4. Values of $\Delta\sigma_H^*$ calculated using $J(0)$ obtained from spectral density mapping *vs* $\Delta\sigma_H^*$ calculated using Eq. [17].

values is immediately apparent. Linear regression yields a slope of 0.944 ± 0.002 with a correlation factor of 0.99. Scatter along the horizontal axis may result from local variations in the magnitude or θ_N angle of the ^{15}N CSA tensors. Neglect of the $J(\omega_N)$ term should lead to a systematic decrease of the $\Delta\sigma_H^*$ calculated using Eq. [17], which would be reflected in the slope. For savinase we find that $J(\omega_N)$ is approximately 8% of $J(0)$, resulting in a 6% systematic underestimate of $\Delta\sigma_H^*$ calculated using Eq. [17], in exact agreement with the slope of the fit of Fig. 4. The measured values of $\Delta\sigma_H^*$ fall in the range 1–25 ppm for savinase, which compares well with the range of 5–25 ppm measured earlier for the HU protein of *Bacillus stearothermophilus* (*1*).

In conclusion, we presented a new experiment that yields high-quality data which can be used for quantitative measurement of the ^{15}N CSA/DD cross-correlation rates. Although it is to be expected that the experiment of Tjandra *et al.* (*13*) would yield data of similar quality, the present experiment allows extraction of these rates from simple linear buildups. The ^{15}N CSA/DD cross-correlation rates, in combination with the $^1H^N$ CSA/DD cross correlation rates, can be used to calculate $\Delta\sigma_H^*$ in a straightforward fashion. The values obtained using this procedure are in excellent agreement with the results obtained using $J(0)$ derived from reduced spectral density mapping. Thus, the method presents a straightforward way for obtaining information about the amide-proton CSA, a quantity correlated with the formation of secondary structural elements and hydrogen bonding.

ACKNOWLEDGMENTS

The authors thank Rob Kaptein for his stimulating interest. We also thank Rick Bott (Genencor, Palo Alto) and Dick Schipper (Gist-Brocades, Delft) for providing the ^{15}N-labeled enzymes. G.W.V. has been financially supported by the Royal Netherlands Academy of Arts and Sciences. This work was supported by the Netherlands Foundation for Chemical Research (SON) with financial assistance from the Netherlands Organization for Scientific Research (NWO).

REFERENCES

1. M. Tessari, H. Vis, R. Boelens, R. Kaptein, and G. W. Vuister, *J. Am. Chem. Soc.,* in press.
2. C. H. Wu, A. Ramamoorthy, L. M. Gierasch, and S. J. Opella, *J. Am. Chem. Soc.* **117,** 6148 (1995).
3. R. Gerald II, T. Bernhard, U. Haeberlen, J. Rendell, and S. J. Opella, *J. Am. Chem. Soc.* **115,** 777 (1993).
4. A. Ramamoorthy, L. M. Gierasch, and S. J. Opella, *J. Magn. Reson. B* **109,** 112 (1995).
5. B. Berglund and R. W. Vaughan, *J. Chem. Phys.* **73,** 2037 (1980).
6. H. M. J. McConnell, *J. Chem. Phys.* **25,** 709 (1956).
7. E. L. Mackor and C. MacLean, *Prog. NMR Spectrosc.* **3,** 129 (1967).
8. M. Goldman, *J. Magn. Reson.* **60,** 437 (1984).
9. S. Wimperis and G. Bodenhausen, *Mol. Phys.* **66,** 897 (1989).
10. R. Bruschweiler and R. R. Ernst, *J. Chem. Phys.* **96,** 1758 (1992).
11. I. Burghardt, R. Konrat, and G. Bodenhausen, *Mol. Phys.* **75,** 467 (1992).
12. L. G. Werbelow, *in* ''Encyclopedia of Nuclear Magnetic Resonance'' (D. M. Grant and R. K. Harris, Eds.), pp. 4072–4078, Wiley, London (1996).
13. N. Tjandra, A. Szabo, and A. Bax, *J. Am. Chem. Soc.* **118,** 6986 (1996).
14. O. W. Sørensen, G. W. Eich, M. H. Levitt, G. Bodenhausen, and R. R. Ernst, *Prog. NMR Spectrosc.* **16,** 163 (1983).
15. L. E. Kay, P. Keifer, and T. Saarinen, *J. Am. Chem. Soc.* **114,** 10663 (1992).
16. F. Delaglio, S. Grzesiek, G. W. Vuister, G. Zhu, J. Pfeifer, and A. Bax, *J. Biomol. NMR* **6,** 277 (1995).
17. M. L. Remerowski, H. A. M. Pepermans, C. W. Hilbers, and F. J. M. Van de Ven, *Eur. J. Biochem.* **235,** 629 (1996).
18. A. J. Shaka, J. Keeler, T. Frenkiel, and R. Freeman, *J. Magn. Reson.* **52,** 334 (1983).
19. C. Betzel, S. Klupsch, G. Papendorf, S. Hastrup, S. Branner, and K. S. Wilson, *J. Mol. Biol.* **223,** 427 (1992).